Kinetic and Thermodynamic Studies of Tet Repressor−Tetracycline Interaction †

ARTICLE *in* BIOCHEMISTRY · FEBRUARY 2005

Impact Factor: 3.02 · DOI: 10.1021/bi048548w · Source: PubMed

4 AUTHORS, INCLUDING:

Sylwia Kędracka-Krok
Jagiellonian University
33 PUBLICATIONS **302** CITATIONS
SEE PROFILE

Andrzej Górecki
Jagiellonian University
24 PUBLICATIONS **170** CITATIONS
SEE PROFILE

Piotr Bonarek
Jagiellonian University
18 PUBLICATIONS **164** CITATIONS
SEE PROFILE

Kinetic and Thermodynamic Studies of Tet Repressor−Tetracycline Interaction†

Sylwia Kedracka-Krok, Andrzej Gorecki, Piotr Bonarek, and Zygmunt Wasylewski*

Department of Physical Biochemistry, Faculty of Biotechnology, Jagiellonian University, Krakow, Poland

Received July 9, 2004; Revised Manuscript Received October 12, 2004

ABSTRACT: Stopped-flow measurements have been employed to study the kinetics of the conformational changes in TetR (B) induced by tetracycline binding with and without Mg^{2+} ions. Result of stopped-flow fluorometry measurements at pH 8.0 indicate conformational changes in the helix−turn−helix motif in the N-terminal domain and in the C-terminal inducer binding domain. Binding of tetracycline (Tc) to TetR in the absence of Mg^{2+} can be described by a simple kinetics process, which is limited to the first step association without any unimolecular conformational change step upon Tc binding. The rate constants for this process are equal to 2.0×10^5 M^{-1} s^{-1} and 2.1 s^{-1} for the forward and backward reaction, respectively, and gave the binding constant $K_a = 0.96 \times 10^5$ M^{-1}. The kinetics of $[Tc-Mg]^+$ binding to TetR can be described by reactions in which the first step describes the association characterized by the rate constants $k_a = 1.4 \times 10^5$ M^{-1} s^{-1} and $k_d = 2.2 \times 10^{-2}$ s^{-1} and binding constant $K_a = 6.3 \times 10^6$ M^{-1}. The first step of $[Tc-Mg]^+$ association is followed by at least three conformational change steps, which occur in the inducer binding site and then propagate to the surroundings of Trp75 and Trp43 residues. The rate constants for the forward, k_c, and backward, k_{-c}, reaction for each of these conformational steps have been determined. The thermodynamics of the binding of tetracycline with and without Mg^{2+} to TetR was investigated by isothermal titration calorimetry (ITC) at pH 8.0 and 25 °C. The measurement shows that TetR dimer possesses two equivalent binding sites for tetracycline, characterized by binding constant $K_a = 9.0 \times 10^6$ M^{-1} and $K_a = 7.0 \times 10^4$ M^{-1} for Tc with and without Mg^{2+}, respectively. The binding of the inducer to TetR, in the presence and absence of Mg^{2+} ion, is an enthalpy-driven reaction characterized by $\Delta H = -51$ kJ mol^{-1} and $\Delta H = -33$ kJ mol^{-1}, respectively. The entropy change, ΔS, for the interaction in the presence of Mg^{2+} is equal to -38.9 J K^{-1} mol^{-1}, and for the tetracycline alone, it was estimated at -17.6 J K^{-1} mol^{-1}.

Resistance to tetracycline in bacteria is negatively regulated by $[Tc-Mg]^+$ complex. The mechanism of this phenomenon is based on the active transport of tetracycline by the antiporter protein TetA. Expression of the *tetA* gene is strictly regulated by Tet repressor. When the tetracycline diffuses into bacteria, it is chelated by divalent metal ions, preferentially by Mg^{2+}, and then undergoes association with a ribosomal subunit and in consequence blocks protein biosynthesis (*1*, *2*). Tet repressor, in the absence of Tc, binds to the *tetO* DNA operator and prevents the transcription of the genes encoding TetR[1] and TetA proteins. The equilibrium association constant of Tc to 30S ribosomal subunit is on the order of 10^6 M^{-1}, which is lower than the association constant of $[Tc-Mg]^+$ with Tet repressor (*3*). Only $[Tc-Mg]^+$ complex is able to trigger the mechanism of conformational changes for induction of Tet repressor but not the tetracycline molecule without the coordinated Mg^{2+} ion (*4*). Binding of tetracycline to TetR at pH 8.7 has been studied by fluorescence measurements (*5*) and the binding constant has been estimated at about 10^9 M^{-1}. The high affinity of TetR to *tetO* operators is drastically diminished upon binding of $[Tc-Mg]^+$ inducer to the protein. This phenomenon is also often used as a controllable switch for the regulation of gene expression in eukaryotes (*6*).

Tet repressor is a homodimer protein, and a crystal structure of TetR(D), with and without the inducer, has been established (*7*, *8*). Each of the identical monomers of TetR is composed of two distinct domains. The N-terminal domain of the protein is responsible for DNA binding by the HTH motif, and the regulatory C-terminal domain has tunnel-like cavities responsible for the inducer binding. The two $[Tc-Mg]^+$ inducer molecules in the dimer of TetR are buried in the binding cavities, and they are about 33 Å apart from the DNA recognition helices. The X-ray structure shows (*8*) that binding of $[Tc-Mg]^+$ inducer into TetR is accompanied by conformational changes in the protein, which in turn abolish its specific interaction with DNA operators. The sequence of conformational changes, triggered by the inducer, starts with conformational changes within amino acids engaged in hydrophobic interactions with tetracycline and closing the entrances of the tunnel. The Mg^{2+} is coordinated by His100 and forms hydrogen bonds with two water molecules. Superposition of the structures of TetR with and without $[Tc-Mg]^+$ shows the pendulum-like movement that shifts HTH motifs in opposite directions. In consequence, the

† This study was partly supported by Grant No. 3P04A00624 from the Ministry of Science and Informatics.

* Corresponding author. Mailing address: Department of Physical Biochemistry, Faculty of Biotechnology, Jagiellonian University, Gronostajowa 7 Str., 30-387 Krakow, Poland. E-mail: wasylewski@mol.uj.edu.pl. Fax: (48 12) 66 46 902.

[1] Abbreviations: TetR, tetracycline repressor; Tc, tetracycline; HTH, helix−turn−helix motif; ITC, isothermal titration calorimetry.

10.1021/bi048548w CCC: $30.25
Published on Web 12/31/2004

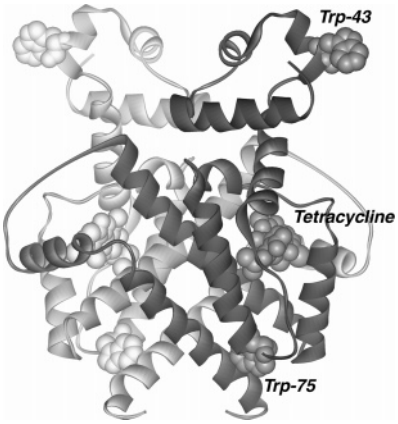

FIGURE 1: Structure of the complex formed between Tet repressor and tetracycline−Mg^{2+}. The locations of tryptophan residues and tetracyclines are marked. The figure was generated with WEBLAB VIEWERPRO (version 3.7) using atomic coordinates for the TetR−tetracycline complex. The coordinates were obtained from Brookhaven Protein Data Bank (accession code 2TCT).

distance between two DNA-binding domains of TetR, measured for the midpoints of the DNA recognition helices of HTH, increases from 36.6 to 39.6 Å (*8*). This distance is too far for recognition of two major grooves of B-DNA by TetR−$[Tc-Mg]^+$ and the protein dissociates from the *tetO* DNA operator and in consequence allows RNA polymerase for induction of expression of *tetR* and *tetA* genes.

Previous biochemical and biophysical studies of Tet repressor were focused on the conformational changes accompanying binding of $[Tc-Mg]^+$ to TetR, both in the crystal phase (*8*) and in solution (*3*, *5*, *9*). In this investigation, we would like to present the results of fast kinetics measurements of tetracycline-induced conformational changes in TetR. In this study, we will use the single tryptophan containing mutants of TetR, which possess Trp43 or Trp75. These tryptophan residues have been used as an intrinsic fluorescent probe, which allows for investigation of TetR conformational changes as the kinetic process upon the inducer binding. We will also use the changes in fluorescence of tetracycline upon binding to the protein to follow the reaction. Since the Trp43 residue is exclusively located in the recognition helix of the HTH motif (Figure 1), this residue can provide the kinetic information about what occurs in N-terminal domain upon the inducer binding. On the other hand, the fluorescence of tetracycline, as well as the Trp75 residue, can inform us about the kinetics of conformational changes occurring in C-terminal domain of TetR. In this study, the thermodynamic parameters, such as binding constant, enthalpy, and entropy changes, characterizing the reactions of tetracycline binding to TetR with and without Mg^{2+}, are determined by isothermal titration calorimetry (ITC). It is shown that when the more complete thermodynamics of the binding reaction are considered, the differences in the interaction of tetracycline and $[Tc-Mg]^+$ with TetR can be described.

MATERIALS AND METHODS

Materials. Acrylamide, phenylmethylsulfonyl fluoride (PMSF), tetracycline, and Tris were purchased from Sigma. Dithiotreitol (DTT), magnesium chloride hexahydrate, and sodium chloride were from Fluka. The Fractogel EMD SO_3^- 650 (M) was from Merck, while Q-Sepharose Fast Flow and Sephacryl S-200 HR were from Amsterdam Pharmacia Biotech. The nutrients for bacterial growth were from Life Technologies. All other chemicals were products of analytical grade from POCh-Gliwice. Buffers in water purified by the Millipore system were used throughout this work.

Protein Purification. The wild-type Tet repressor, TetR (B), and single tryptophan mutants TetR W43 and TetR W75 were overproduced in *Escherichia coli* strain RB 791. These bacterial strains were a kind gift from Prof. W. Hillen (Universitat Erlangen-Nurnberg, Germany). Protein purification in general followed the scheme described by Ettner et al. (*10*) with a few modifications (*11*). After the purification procedure, the protein was highly pure (>97%) as judged by SDS−polyacrylamide gel electrophoresis and Coommasie brilliant blue staining. The concentration of the dimer TetR variants was determined spectrophotometrically using excitation coefficients $\epsilon_{280nm} = 30 \times 10^3$ (*12*), 22×10^3 (*13*), and 20.7×10^3 M^{-1} cm^{-1} estimated from amino acid sequence (*14*) for TetR wt, TetR W43, and TetR W75, respectively. The activity of the proteins was checked using the tetracycline titration method. Concentration of tetracycline was determined in 0.1 M HCl using an excitation coefficient of $\epsilon_{355nm} = 13\,320$ M^{-1} cm^{-1} (*5*). The measurements were performed in buffer A, 10 mM Tris, 150 mM NaCl, and 2 mM DTT with 10 mM $MgCl_2$, pH 8.0, or in the absence of Mg^{2+} ion in buffer B, 10 mM Tris, 150 mM NaCl, and 2 mM DTT with 1 mM EDTA, pH 8.0.

Stopped-Flow Fluorescence Measurements. Kinetic experiments were performed on a SX-17 MV stopped-flow spectrophotometer from Applied Photophysics (United Kingdom) in two syringes mode at 25 ± 0.2 °C. The dead time of mixing was determined to be less than 2 ms. Changes in the protein conformation induced by Tc binding were monitored in two different ways: (1) the increase in Tc fluorescence was observed through a 475 nm cutoff filter (475FG03−25) from Andover Corporation with excitation at 370 nm; (2) the decrease in Tet repressor fluorescence was detected using band-pass filter 001FG09-25 from Andover Corporation with maximum transmittance at 360 nm with excitation at 295 nm. For both types of experiments, two different series of measurements were performed, the first with large excess of one of reagents and the second with concentration of substrates close to equimolar. The mixing volume ratio was always 1:1. Four thousand data points were acquired in each stopped-flow trace, and background measurements were carried out at the beginning of each experiment. Ten to fourteen kinetic traces were averaged to obtain adequate signal-to-noise ratios. In case of experiments with excess of one of the reagents, that is, under pseudo-first-order conditions in which the concentration of binding sites of one substrate was 4−60-fold greater than that of the second one, averaged kinetic traces were fit using software supplied by Applied Photophysics to a single-exponential decay or to a sum of such terms

$$F(t) = \Delta F \exp(-k_{obs}t) + F_\infty \qquad (1)$$

where F is the fluorescence intensity at time t, ΔF and k_{obs} are the amplitude and observed rate constant, respectively, and F_∞ is the fluorescence at infinite time. The validity of the fitting was evaluated by an inspection of residuals and normalized variation parameters.

In case of semiequimolar substrate concentrations, sets of progress curves were simultaneously fitted to an arbitrary reaction mechanism represented symbolically by a set of chemical equations using the DynaFit program (*15*). The program determines the set of differential equations and then uses iterative nonlinear regression analysis to determine the best-fit parameters to the experimental data. The estimated parameters were rate constants, molar fluorescence responses of each compound, concentrations of protein, and offset of traces. The program was used to analyze the reaction by considering several alternate reaction mechanisms. To determine the appropriate model, a few criteria were used: (1) inspection of independent and dependent residuals; (2) convergence of the estimated parameters obtained from fitting of independent sets of traces at different concentrations of unchanged compound; (3) statistical criteria, that is, sum of squares and *F* statistic; (4) convergence of the estimated rate constants obtained from global analysis and pseudo-first-order kinetics; (5) convergence of the calculated equilibrium association constants obtained from global analysis and ITC measurement. For each type of experiments, two sets of progression curves were measured. In each set, the concentration of a reactant, the fluorescence of which was measured, was fixed. The two sets of kinetic traces were performed at different concentrations of this reactant. For each experiment, a few types of reaction mechanisms were considered. Two sets of data were fitted independently. For the appropriate model, kinetic constants were convergent.

To choose the appropriate model, we have used the *F* statistical test (*16*). Parameters *F* have been calculated by the following equation:

$$F = \frac{(S_1 - S_2)}{S_2}\frac{(n - p_1)}{(p_2 - p_1)} \qquad (2)$$

where n is the number of data points, S_1 and S_2 are the sums of squares in models 1 and 2, respectively, and p_1 and p_2 are the numbers of fitted parameters in models 1 and 2. To distinguish between the simpler model 1 and the more complicated model 2, the critical values of F_{crit}, calculated at the 95% confidence level, have been compared with the appropriate *F* values. When the *F* value was lower then the appropriate value of F_{crit}, the simpler model 1 has been accepted.

Isothermal Titration Calorimetry. All calorimetric experiments were performed with a VP−ITC MicroCalorimeter (MicroCal, Inc., Northampton, MA) in the buffer A, with or without Mg^{2+} cation, at 25 °C. All solutions were thoroughly degassed under vacuum for 5 min before being used. Ligand (tetracycline) was prepared in the dialysate of the protein buffer to minimize artifacts due to different compositions of solutions. The reaction cell contained 1.4355 mL of protein in buffer, and the reference cell contained distilled water only. The injection syringe was filled with ligand solution and rotated at 300 rpm during equilibration and experiment. Titration experiments consisted of 20−45 injections. The volume of the first injection was 3 μL, and the subsequent injection volumes were 3 and 5 μL for experiments with and without Mg^{2+}, respectively. Injection speed was 0.5 μL/s with 4-min intervals between injections. For experiments in the absence of Mg^{2+}, separate titrations of the ligand solution in the buffer were performed to determine the heat of ligand dilution. For titrations in the presence of Mg^{2+}, the additions were continued 5−6 times past saturation so that a heat of ligand dilution could be determined from these additional peak areas. The heats of dilution obtained from both cases were then subtracted from the heats obtained during the titration, prior to analysis of the data.

A Leverber−Marquardt algorithm performed by MicroCal Origin scientific plotting software was used to fit the incremental heat of the *i*th titration [$(\Delta Q(i)$] of the total heat, Q_t

$$\Delta Q(i) = Q(i) + \frac{dV_i}{V_0}\left[\frac{Q(i) + Q(i-1)}{2}\right] - Q(i-1) \qquad (3)$$

where V_0 is the volume of the sample solution. For the model of the single set of identical independent sites, the following equation was used:

$$Q_t = \frac{n[\mathrm{P}]_t \Delta H_b V_0}{2}\left[1 + \frac{[\mathrm{L}]_t}{n[\mathrm{P}]_t} + \frac{1}{nK[\mathrm{P}]_t} - \sqrt{\left(1 + \frac{[\mathrm{L}]_t}{n[\mathrm{P}]_t} + \frac{1}{nK[\mathrm{P}]_t}\right)^2 - \frac{4[\mathrm{L}]_t}{n[\mathrm{P}]_t}}\right] \qquad (4)$$

where n is the stoichiometry of the binding reaction, $[\mathrm{P}]_t$ is the total TetR concentration in the sample vessel, H_b is the binding enthalpy, and K_b is the binding constant. The binding entropies, S_b, were calculated using the following equation of the thermodynamics:

$$\Delta S_b = (\Delta H_b - \Delta G_b)/T \qquad (5)$$

Standard deviations for H_b, S_b, and K_b were calculated from multiple titration runs.

RESULTS

Kinetics Measurements. The kinetics of the binding of tetracycline to the TetR was measured as changes in the tetracycline fluorescence intensity using a stopped-flow method with fixed final concentration of tetracycline equal to 1 μM. In all cases, after adding TetR, an increase in tetracycline fluorescence was observed with increasing protein concentration. The data for interaction between TetR and $[\mathrm{Tc-Mg}]^+$ complex were fit to a single-exponential or to a sum-of-exponentials model. In all cases, a double-exponential model was superior, as can be judged from the normalized variance and residual distribution analysis. Addition of a third exponent did not improve the goodness of the fit. The dependence of the rates for the fast and slow process on protein concentration is shown in Figure 2. The data for the faster process were fit to a straight line giving a second-order rate constant, k_a, of $(1.17 \pm 0.02) \times 10^5\ \mathrm{M^{-1}\ s^{-1}}$ and showed no signs of leveling off at the higher protein concentration. The intercept of the straight line with the *y*-axis should give the dissociation rate constant, k_d, but this cannot be reliably distinguished from zero with the obtained data. The second dependence of the rate of the slower process has a hyperbolic shape, which suggests that $[\mathrm{Tc-Mg}]^+$ binding to TetR is followed by protein conformational changes. Unfortunately, the errors of the observed rate constants do not allow for estimation of the elementary rate constant, k_c and k_{-c}, with high accuracy.

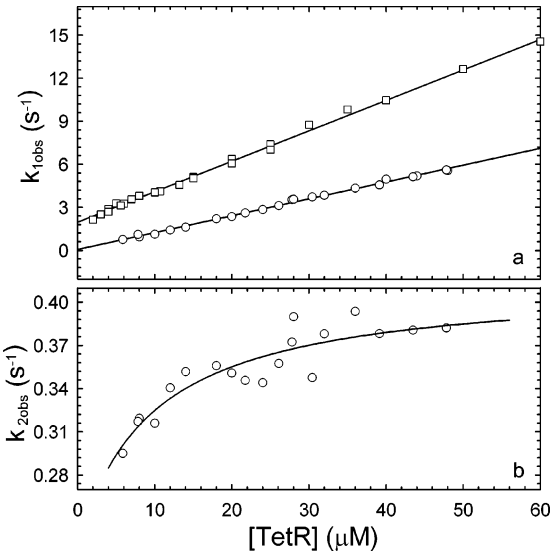

FIGURE 2: Plot showing the dependence of the pseudo-first-order rate constants obtained from experiments of mixing excess of TetR wt with tetracycline. In panel a, the slope of fitted straight line corresponds to apparent second-order rate constants. Symbols ○ mark data in the presence of Mg^{2+} and symbols □ refer to data in the absence Mg^{2+}. Panel b shows the dependence of the observed rate constant for the slower phase of reaction on the concentration of binding sites of TetR wt in the experiment with magnesium ions. The final concentration of tetracycline was 1 μM. Measurements were performed at 25 °C in buffer B in the absence of magnesium or in buffer A in the presence of Mg^{2+}.

In case of interaction between TetR and tetracycline in the absence of divalent metal ion, a single-exponential is sufficient, as can be judged from the statistical analysis of the data, to describe kinetic traces obtained under pseudo-first-order conditions. Figure 2a shows that k_{obs} is linearly related to protein concentration as predicted by equation $k_{obs} = k_a[TetR] + k_d$. The individual rate constants were calculated by linear regression analysis and gave the following values: $k_a = (2.12 \pm 0.02) \times 10^5\ M^{-1}\ s^{-1}$; $k_d = 1.98 \pm 0.06\ s^{-1}$. The equilibrium association constant K_a calculated from k_a and k_d is $(1.07 \pm 0.07) \times 10^5\ M^{-1}$.

The kinetics of the binding of tetracycline to TetR were also analyzed in second-order conditions with the DynaFit computer global analysis program. Usually the global analyses were performed using 19−39 independent traces measured at different ligand concentrations. In Figures 3, 4, and 5, the typical kinetic courses of the reaction of tetracycline alone with TetR wt and its single tryptophan containing mutants, TetR W43 and TetR W75, are shown, respectively. In the case of an interaction between TetR wt and tetracycline, the progress of the reaction was monitored by the changes in fluorescence intensity of tetracycline. In these experiments, the final concentration of TetR wt ranged from 0.5 to 70 μM for both tetracycline concentrations, that is, 1 and 2 μM. In the case of TetR W43 and TetR W75 mutant measurements, the decrease of tryptophan fluorescence of the protein was observed with increasing tetracycline concentration. For each experiment with TetR W43 and TetR W75, where intensity of tryptophan fluorescence was monitored, final concentration of Tc ranged from 0.25 to 15 μM for both protein concentrations, 1 and 2 μM. Progress curves of the reaction of tetracycline in the absence of Mg^{2+} and TetR wt, as well as mutants TetR W43 and TetR W75, were analyzed by the global DynaFit program, in which two

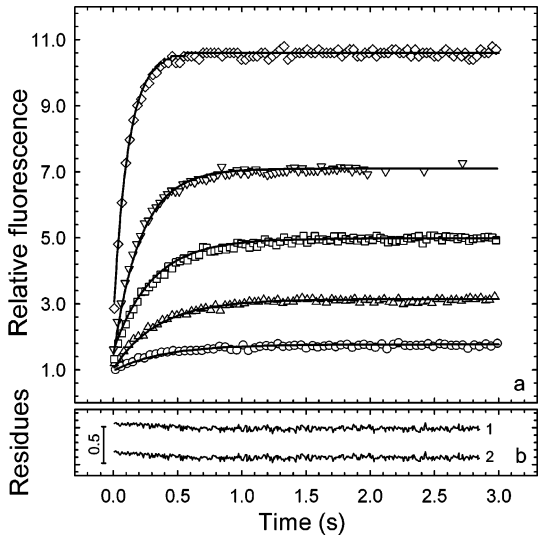

FIGURE 3: Kinetics of tetracycline binding to TetR wt measured by the changes in the fluorescence intensity of Tc (in the absence of Mg^{2+}). Measurements were performed at 25 °C in buffer B, pH 8.0, at Tc final concentration of 1 μM and various TetR final concentrations: (○) 0.95; (△) 2.85; (□) 5.32; (▽) 12.54; (◇) 33.25 μM. The solid lines are the best fit of global analysis obtained from the DynaFit program according to the model described in the scheme in eq 6, characterized by the parameters presented in Table 1. Panel b shows the plots of the residuals, (determined for the data (△) in panel a) for the fit to models 1, described by the scheme in eq 6, and 2, described by the scheme in eq 7 in the text.

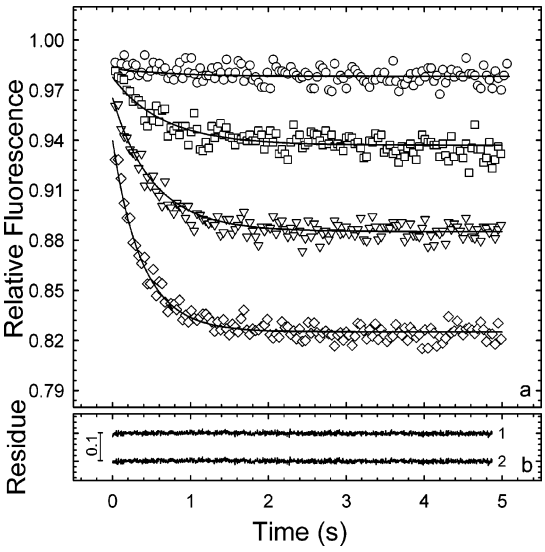

FIGURE 4: Kinetics of tetracycline binding to TetR W43 measured by the changes in the fluorescence intensity of tryptophan residues (in the absence of Mg^{2+}). Measurements were performed at 25 °C in buffer B, pH 8.0, at TetR W43 final concentration of 1.25 μM and various Tc final concentrations: (○) 0.2; (□) 2; (▽) 5; (◇) 10 μM. The solid lines are the best fit of global analysis obtained from the DynaFit program according to the model described in the scheme of eq 6, characterized by the parameters presented in Table 1. Panel b shows the plots of the residuals (determined for the data (◇) in panel a) for the fit to models 1, described by the scheme in eq 6, and 2, described by the scheme in eq 7 in the text.

independent models were considered. The first simple model described the one-step tetracycline binding process to each monomer without consecutive reactions, and the second one described the process in which the binding of tetracycline to TetR wt and its mutants was followed by conformational changes of each monomer of the protein. The best model,

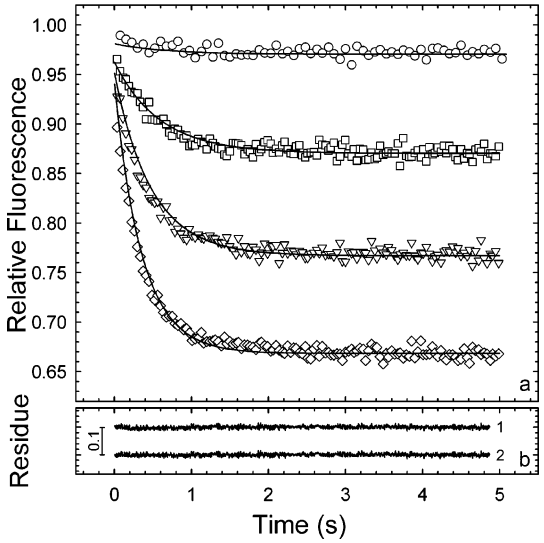

FIGURE 5: Kinetics of tetracycline binding to TetR W75 measured by the changes in the fluorescence intensity of tryptophan residues (in the absence of Mg^{2+}). Measurements were performed at 25 °C in buffer B, pH 8.0, at TetR W75 final concentration of 1.25 μM and various Tc final concentrations: (○) 0.2; (□) 2; (▽) 5; (◇) 10 μM. The solid lines are the best fit of global analysis obtained from the DynaFit program according to the model described in the scheme of eq 6, characterized by the parameters presented in Table 1. Panel b shows the plots of the residuals (determined for the data (▽) in panel a) for the fit to models 1, described by the scheme in eq 6, and 2, described by the scheme in eq 7 in the text.

which described the binding of tetracycline alone to TetR wt as well as its mutants, was one-step ligand binding to each monomer of the protein, according to the scheme in eq 6. This model was superior, as can be judged by the analysis of *F* statistic parameters described by eq 1. The values of the F/F_{crit} ratio, calculated according to the eq 1, are equal to 0.459, 0.916, and 0.465 for TetR wt, TetR W75, and TetR W43, respectively. Since all of these *F* values are lower than F_{crit} values, then one can expect that the simple kinetic model (scheme 6) is sufficient to describe tetracycline binding to TetR and its mutant in the absence of Mg^{2+} ion. This observation can be supported by the visual inspection of the residual distribution presented in Figures 3, 4, and 5, which shows that fitting the experimental data to the more complicated model described by the scheme in eq 7 does not lead to the improved goodness of these fits. Taking together, the best model that described this process was one-step ligand binding to each monomer of the protein, according to the scheme

$$\mathrm{TetR} + \mathrm{Tc} \underset{k_d}{\overset{k_a}{\leftrightarrow}} \mathrm{TetR{-}Tc} \qquad (6)$$

The rate constants and calculated association constant obtained with the DynaFit program are shown in Table 1.

The typical kinetic courses of the binding of $[Tc{-}Mg]^+$ complex to TetR wt are presented in Figure 6. In all cases, the fluorescence of $[Tc{-}Mg]^+$ complex increased after adding of TetR. For each experiment, the final concentration of the protein was in the range from 0.2 to 40 μM in two independent sets of the measurements performed with concentrations of tetracycline equal to 1 or 2 μM. Progress curves of the reaction of tetracycline in the presence of Mg^{2+} and TetR fit very well with the model, as described by global

Table 1: Rate Constants for Association and Dissociation of TetR and Tetracycline in the Absence of Magnesium Ions, Obtained in the Experiment Monitoring the Changes in Fluorescence Emission of Tetracycline and by Detection of the Fluorescence of Tryptophan Residues of Single Tryptophan Mutants[a]

TetR wt + Tc (without Mg^{2+})			
TetR	k_a ($M^{-1}s^{-1}$) × 10^5	k_d (s^{-1})	K_a (M^{-1}) × 10^5
wt[b,d]	2.12 ± 0.02	1.98 ± 0.06	1.07 ± 0.07
wt[c,d]	2.040 ± 0.002	2.130 ± 0.006	0.96 ± 0.05
W75[b,e]	1.52 ± 0.07	1.6 ± 0.1	0.96 ± 0.07
W75[c,e]	1.869 ± 0.004	1.103 ± 0.002	1.694 ± 0.005
W43[b,e]	1.20 ± 0.04	1.43 ± 0.07	0.84 ± 0.05
W43[c,e]	1.71 ± 0.03	0.88 ± 0.01	1.94 ± 0.04

[a] The measurements were performed in buffer B, pH 8.0, at 25 °C. [b] The values of association rate constant obtained by analysis of kinetic traces measured under pseudo-first-order conditions. [c] The values of association rate constant obtained by analysis of kinetic traces measured under second-order conditions and calculated by the DynaFit program. [d] Excitation and emission of tetracycline. [e] Excitation and emission of tryptophan residues.

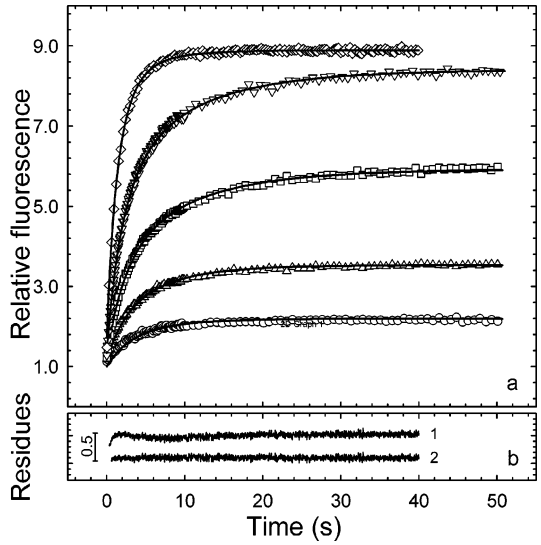

FIGURE 6: Kinetics of tetracycline binding to TetR measured by the changes in the fluorescence intensity of Tc (in the presence of Mg^{2+}). Measurements were performed at 25 °C in buffer A, pH 8.0, at Tc final concentration of 1 μM and various TetR final concentrations: (○) 0.5; (△) 1; (□) 2; (▽) 4; (◇) 8 μM. The solid lines are the best fit of global analysis obtained from the DynaFit program according to the model described in the scheme of eq 7, characterized by the parameters presented in Table 2. Panel b shows the plots of the residuals (determined for the data (◇) in panel a) for the fit to models 1, described by the scheme in eq 6, and 2, described by the scheme in eq 7 in the text.

analysis with the DynaFit program, in which the binding of tetracycline to TetR and Tc was followed by conformational changes of each monomer of the protein, according to the scheme:

$$\mathrm{TetR} + \mathrm{Tc} \underset{k_d}{\overset{k_a}{\leftrightarrow}} \mathrm{TetR{-}Tc} \underset{k_{-c}}{\overset{k_c}{\leftrightarrow}} \mathrm{TetR^*{-}Tc} \qquad (7)$$

This model was superior, as can be judged by the *F* statistic analysis as well as by the visual inspection of the residual distribution plots presented in Figures 6, 7, and 8, for both types of experiments, that is, where progress of reactions was monitored by the changes in tetracycline intensity, as well as in the case when the fluorescence intensity changes of one tryptophan residue of TetR mutants were observed

Table 2: Kinetic Parameters of Interaction of TetR with Tetracycline in the Presence of Magnesium Ions Obtained in Two Types of Experiment, Namely, by Monitoring the Changes in Fluorescence Emission of Tetracycline and by Detection of a Decrease in Fluorescence of Tryptophan Residues of Single Tryptophan Mutants[a]

TetR	k_a[b] (M^{-1} s^{-1}) × 10^5	k_a (M^{-1} s^{-1}) × 10^5	k_d (s^{-1})	K_a (M^{-1}) × 10^6	k_c (s^{-1})	k_{-c} (s^{-1})	K_c
			Excitation and Emission of Tetracycline				
wt	1.17 ± 0.02	1.46 (0.1)	0.019 (1.0)	7.7 (0.9)	0.20 (0.5)	0.010 (1.7)	0.050 (1.2)
			Excitation and Emission of Tryptophan Residues				
W75	1.10 ± 0.04	1.60 (0.4)	0.032 (3.4)	4.9 (3.0)	0.092 (3.7)	0.041 (2.0)	0.45 (1.7)
W43	1.02 ± 0.02	1.17 (0.9)	0.017 (3.8)	6.9 (2.9)	0.072 (0.8)	0.017 (2.0)	0.24 (1.2)

[a] The values were calculated by DynaFit computer program according to the model including two consequent reversible reaction. The measurements were conducted in buffer A, pH 8.0, at 25 °C. The values in the brackets indicate the percent of the error. [b] The values of association rate constant obtained by analysis of kinetic traces measured under pseudo-first-order conditions.

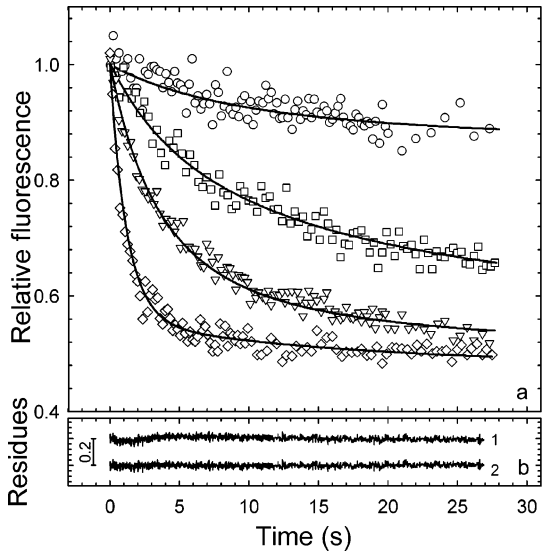

FIGURE 7: Kinetics of tetracycline binding to TetR W43 measured by the changes in the fluorescence intensity of tryptophan residues (in the presence of Mg^{2+}). Measurements were performed at 25 °C in buffer A, pH 8.0, at TetR W43 concentration of 1 μM and various Tc final concentrations: (○) 0.25; (□) 1; (▽) 2.5; (◇) 7.5 μM. The solid lines represent the best fit of global analysis obtained from the DynaFit program according to model described in the scheme in eq 7, characterized by the parameters presented in Table 2. Panel b shows the plots of the residuals (determined for the data (◇) in panel a) for the fit to models 1, described by the scheme in eq 6, and 2, described by the scheme in eq 7 in the text.

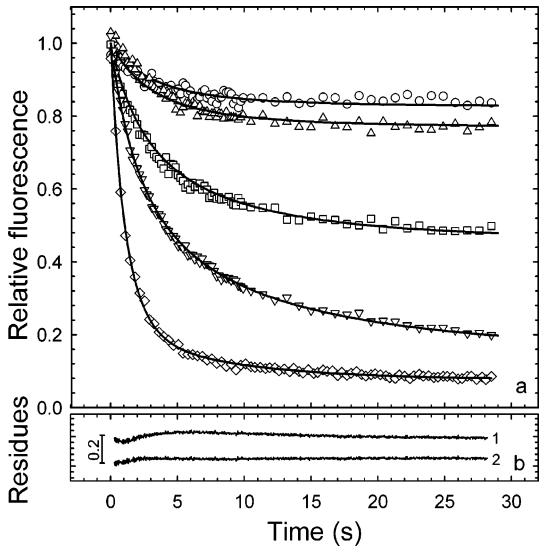

FIGURE 8: Kinetics of tetracycline binding to TetR W75 measured by the changes in the fluorescence intensity of tryptophan residues (in the presence of Mg^{2+}). Measurements were performed at 25 °C in buffer A, pH 8.0, at TetR W75 concentration of 1 μM and various Tc final concentrations: (○) 0.4; (△) 0.5; (□) 1.25; (▽) 2; (◇) 6 μM. The solid lines are the best fit of global analysis obtained from the DynaFit program according to the model described in the scheme in eq 7, characterized by the parameters presented in Table 2. Panel b shows the plots of the residuals (determined for the data (◇) in panel a) for the fit to models 1, described by the scheme in eq 6, and 2, described by the scheme in eq 7 in the text.

upon adding $[Tc-Mg]^+$. The values of F/F_{crit} ratio are equal to 779.5, 1499.5, and 1126.4 determined for TetR wt, TetR W75, and TetR W43, respectively. All these values indicate that the F ratio values are significantly higher than the value of F_{crit} and therefore strongly suggest that in the presence of Mg^{2+} ions the kinetics of tetracycline−TetR interaction can be described by the model presented in scheme 7. This observation is also supported by the residual distribution presented in Figures 6, 7, and 8, which clearly shows that the goodness of the fits is better in the case of the model described by Scheme 7. In each case, after adding tetracycline, the decrease of the tryptophan fluorescence of the protein was observed with increasing ligand concentration. The decrease of fluorescence intensity was significantly more pronounced in the case of TetR W75 than in the case of TetR W43. The rate constants and associated equilibrium constants obtained from global analysis are presented in Table 2. For each experiment where intensity of tryptophan was monitored, final concentration of Tc was in the range from 0.25 to 15 μM for both protein concentrations, 1 and 2 μM.

Thermodynamic Measurements. The typical results of ITC titrations of TetR wt solution with tetracycline solution in the absence and presence of Mg^{2+} are shown in Figures 9 and 10, respectively. In both cases, the titration solution containing about 2 mM tetracycline was added to about 50 μM TetR solutions. The titrations were performed at 25 °C. The titrations were continued until there were not significant changes in peaks areas. The average parameters of fits of the data to eq 3 are presented in Table 3. Each parameter for all binding reactions in Table 3 is an average determined from at least two different titration runs. The stoichiometry of the binding reactions was always close to two (about 1.7 for TetR wt with and without Mg^{2+}). Both tetracycline binding reactions were exothermic with binding enthalpies equal to -32.9 ± 1.05 kJ mol^{-1} for TetR wt without Mg^{2+} and equal to -51.5 ± 2.05 kJ mol^{-1} for TetR wt with Mg^{2+}. An unfavorable, negative change in entropy was observed in the binding reaction (-17.6 ± 3 and -38.9 ± 5.3 J mol^{-1} K^{-1} for conditions without and with Mg^{2+}, respectively). The interaction between tetracycline and TetR wt is solely driven by a decrease in the enthalpy.

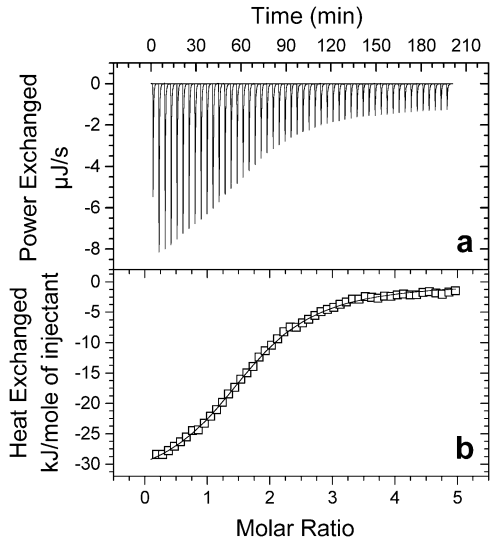

FIGURE 9: Panel a shows the ITC titration of 50 μM TetR wt with 3 μL aliquots of 2.26 mM tetracycline in the absence of Mg^{2+} in buffer B, pH 8.0, at 25 °C. Panel b shows the binding isotherm for titration as described in panel a where the solid line is the best fit of the data to a one-site binding model.

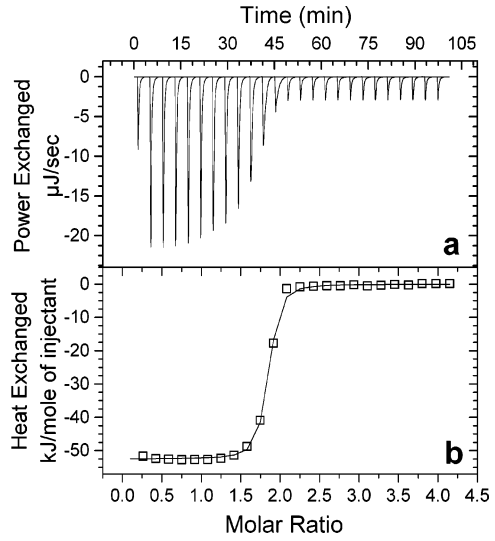

FIGURE 10: Panel a shows the ITC titration of 43.5 μM TetR wt with 5 μL aliquots of 2.02 mM tetracycline in the presence of Mg^{2+} in buffer A, pH 8.0, at 25 °C. Panel b shows the binding isotherm for titration as described in panel a where the solid line is the best fit of the data to a one-site binding model.

Table 3: Thermodynamic Parameters for Tetracycline Binding to Tetracycline Repressor (in the Absence and the Presence of Mg^{2+})[a]

parameters	TetR wt + Tc	TetR wt + [Tc−Mg]$^+$
K_a (M^{-1})	$(6.99 \pm 0.49) \times 10^4$	$(9.05 \pm 1.20) \times 10^6$
ΔH (kJ mol^{-1})	-32.93 ± 1.05	-51.5 ± 2.05
ΔS (J K^{-1} mol^{-1})	-17.64 ± 3.02	-38.92 ± 5.32

[a] All measurements were performed at 25 °C in buffer B, pH 8.0, in the absence of magnesium and in buffer A, pH 8.0, in the presence of Mg^{2+}.

The differences between binding constants are more significant and range from $(6.99 \pm 0.49) \times 10^4$ M^{-1} for TetR without Mg^{2+} to $(9.05 \pm 1.2) \times 10^6$ M^{-1} for TetR wt with Mg^{2+}. Although the presence of divalent cations induces the decrease in entropy, the greater negative change of enthalpy is observed.

DISCUSSION

In this study, the stopped-flow method and titration calorimetry have been used to observe the kinetic and thermodynamic mechanism of TetR−Tc interaction. Binding of tetracycline, in complex with Mg^{2+} ions, leads to drastic changes both in fluorescence of tetracycline and in the intrinsic fluorescence of tryptophan residues. The kinetic measurements have been performed by observation of changes in tetracycline fluorescence, as well as by changes in the fluorescence of single tryptophan containing mutants, which possess only Trp43 or Trp75 residues. However in the absence of Mg^{2+} ions, the observed changes are much less pronounced. The fluorescence of tetracycline was used to study the kinetics of conformational change within surroundings of the protein upon binding the inducer. The process was studied under pseudo-first-order conditions, as well as using direct global analysis of the kinetic data to the second-order reaction, analyzed by the DynaFit program (*15*). Under pseudo-first-order kinetics, in the case of binding of tetracycline alone, the process can be described by a simple exponential. The rates of the observed process linearly increased with the rising ligand concentrations. The direct analysis, without any preassumption performed by the DynaFit program gave the best fit to the same simple model based on the results obtained from pseudo-first-order kinetics measurements. The rate constants k_a and k_d and the association constant K_a are in good agreement with these found in pseudo-first-order reaction and give further support to the observation that the binding of tetracycline alone to TetR can be described by a simple association process, without any unimolecular conformational change step upon Tc binding. On the other hand, for analysis of the kinetic data in pseudo-first-order conditions, two exponentials are required to describe the kinetics of [Tc−Mg]$^+$ complex binding to TetR. The rate of the faster process increased with the [Tc−Mg]$^+$ inducer and gave the association rate constant k_a equal to 1.17×10^5 M^{-1} s^{-1}. The rate of the slow process increased with increasing ligand concentration, reaching an asymptotic value at a molar ratio of TetR/[Tc−Mg]$^+$ higher than 100 μM. Such behavior is usually interpreted as a two-step sequential kinetic process, where the association step is followed by unimolecular change step (*17*). Unfortunately, because of much lower fluorescence intensity changes of [Tc−Mg]$^+$ at higher protein concentration in the case of slow step and also because more independent parameters are needed in the fitting procedure, the only qualitative information can be drawn from the analysis of this process. Nevertheless, using the computer DynaFit program, we were able to describe kinetics of TetR−[Tc−Mg]$^+$ interaction. It should be emphasized that few fitting terms were utilized to describe the stopped-flow data sets. These parameters were recovered from several different stopped-flow traces, which gave about 50 000 data points. The unknown parameters in the fitting procedure were linked over all of the stopped-flow data sets. The rigorous statistical data analysis has shown that the best model can be described by sequential reversible process as proposed by measurements under pseudo-first-order conditions. The consistence of the recovered kinetic parameters obtained from the independent pseudo-first-order measurements as well as from the global

analysis, gives a high confidence of the proposed kinetic model of TetR−tetracycline interaction.

For simplicity of analysis, it has been assumed that the two binding sites for tetracycline in the protein dimer are identical and independent, and in consequence, all of the fitting procedures were performed for the monomeric form of the protein. This assumption is reasonable since it is well-known that the two Tc binding sites in TetR dimer are not cooperative (*5*). The data analysis of the unimolecular conformational change step gave the rate constant $k_c = 0.2$ s^{-1} and $k_{-c} = 0.01$ s^{-1}, which allow calculation of the equilibrium constant between Tet repressor before and after the conformational change, at least in the surroundings of Tc binding site. The low value of $K_c = 0.05$ indicates that TetR bound to $[Tc-Mg]^+$ has been switched into the active conformation.

There are two tryptophan residues, Trp43 and Trp75, in each Tet repressor subunit. From the X-ray structure (*8*), it is known that Trp43 is located about 3 nm from the center of tetracycline and Trp75 is closer, 1.7 nm from the inducer located in the protein pocket. The Trp43 residue is exclusively located in the helix−turn−helix motif in the N-terminal domain of the protein, and the changes in its fluorescence intensity induced upon binding of Tc into hydrophobic pocket in C-terminal domain of Tet repressor can give the information about the kinetic mechanism of cross-talk between these two domains. On the other hand, changes in fluorescence of tetracycline and the Trp75 residue give the information about the changes in the protein in the surroundings of these species in the C-terminal domain upon TetR−Tc complex formation.

To determine the kinetic mechanism of the interaction of $[Tc-Mg]^+$ with TetR, the stopped-flow measurements were performed and monitored using single tryptophan containing mutants, which possess either the Trp43 or Trp75 residue. The process was studied both under pseudo-first-order conditions and in conditions of second-order reaction and analyzed by the DynaFit computer program.

Interaction of tetracycline with TetR leads to a decrease in Trp43 and Trp75 fluorescence intensity and to a substantial increase in the fluorescence of tetracycline; however, these changes are much more pronounced in the presence of Mg^{2+} than in the case of Tc alone. Upon binding of $[Tc-Mg]^+$ complex to TetR, the fluorescence of Trp43 decreased, which in part can result from the energy transfer from Trp43 to the tetracycline, with the concomitant blue shift in the fluorescence emission maximum by about 10 nm. Our previous studies also indicate that binding of $[Tc-Mg]^+$ complex into TetR induces changes of several other fluorescence parameters, such as the decrease in Trp43 fluorescence lifetime (*18*), quenching of its emission by iodide quencher (*9*), and fluorescence anisotropy changes (*19*, *20*) of Trp43 residue. The observed changes can be explained by a decrease in internal mobility and hydrophobicity of the Trp43 residue, as well as by changes in distance between this residue located in the HTH motif in the N-terminal domain and tetracycline located in C-terminal domain of the protein. The fluorescence emission of the Trp43 residue of TetR was used to study the kinetics of the conformational change of the HTH motif, as well as the distance between both domains of the protein due to tetracycline binding to TetR. The kinetic process was studied under pseudo-first-order conditions, and in all cases, it was well described by two exponentials. The rate of the observed process, calculated for the first fast exponent, linearly increased with increasing $[Tc-Mg]^+$, which indicated the ligand binding step. The slower process, described by the second relaxation time, shows a hyperbolic shape of the plot of k_{obs} versus the inducer concentration. The data analysis by DynaFit program in the conditions of second-order reaction gave the best fit to the same model as described by tetracycline fluorescence changes in the case of $[Tc-Mg]^+$ binding. The rate association constant remains in reasonable agreement with the value estimated from pseudo-first-order measurements (Table 2). The dissociation rate constant, calculated for TetR mutant containing Trp43, is very close to the value of k_d determined for TetR wt, obtained upon the observation of changes in $[Tc-Mg]^+$ fluorescence intensity. The association constant K_a calculated from the rate constants of TetR W43 mutants is equal to 6.9×10^6 M^{-1}. The unimolecular conformational change step, which occurs in the surroundings of Trp43 residue, can be described by the rates $k_c = 7.2 \times 10^{-2}$ s^{-1} and $k_{-c} = 1.7 \times 10^{-2}$ s^{-1}, which gave equilibrium constant $K_c = 0.24$ between TetR before and after conformational changes. This value is significantly higher than the K_c value determined for the transition in the surroundings of tetracycline binding pocket and can indicate that this equilibrium is less shifted into the active conformation of TetR. The comparison of the k_c values can indicate that the isomerization step, which involves the HTH structure of TetR, occurs with higher relaxation time than the relaxation time of conformational changes, which occur in the protein surroundings of Tc.

To determine the kinetic mechanism of conformational changes in C-terminal domain of TetR caused by $[Tet-Mg]^+$ binding, the stopped-flow measurements were performed by observation of the TetR Trp75 residue fluorescence intensity changes using single tryptophan containing mutant. The process was studied under pseudo-first-order conditions, and similarly to the results obtained in the case of Trp43-containing TetR, is well described by two exponents. We have also studied this process under second-order conditions and analyzed the kinetic data by DynaFit program. The results presented in Table 2 show that the fast process, described by association rate constant k_a, remains in good agreement with the values of association rate k_a determined by observation of tetracycline fluorescence changes upon binding to the protein. It is well-known (*18*) that the fluorescence of the Trp75 residue of TetR is effectively quenched by fluorescence energy transfer mechanism upon binding of the inducer. It can be expected that this phenomenon should be more visible in the case of Trp75 then for the Trp43 residue since the distance of Trp75−Tc in the TetR complex is about 1.7 nm in comparison to the distance of about 3.0 nm that has been found for the pair Trp43−Tc (*8*). The equilibrium constant, K_a, calculated for the TetR W75 mutant is in the range of the K_a values determined for the TetR wt, as well as the mutant TetR W43 (Table 2). The consistency of these kinetic and thermodynamic parameters strongly supports the suggestion that the fast process, independently of the use of fluorescence emitting species for the reaction progress observations, monitors the association of the inducer with the protein. This phenomenon, in the case of binding of $[Tc-Mg]^+$ complex into Tet repressor,

is followed by at least three conformational change steps, which occur in the inducer binding site and then propagate in the surroundings of the Trp75 residue located in the C-terminal domain and in the surroundings of the Trp43 residue in N-terminal domain of the protein. All these changes can be described by their own values of rate constants k_c and k_{-c}, as well as by the equilibrium constant K_c between Tet repressor before and after the conformational changes. The different values of K_c calculated for each step indicate that almost all Tet repressor molecules bound to $[Tet-Mg]^+$ will be in the active conformation of the inducer pocket, in opposition to the next steps, which differ in equilibrium between active and inactive conformations. Taking these together, we would like to suggest that the kinetics of the interactions of $[Tc-Mg]^+$ inducer complex with Tet repressor can be described by the following consecutive reversible reactions:

$$\mathrm{TetR} + \mathrm{Tc} \underset{k_d}{\overset{k_a}{\leftrightarrow}} \mathrm{TetR{-}Tc} \underset{k_{-c_1}}{\overset{k_{c_1}}{\leftrightarrow}} \mathrm{TetR^{*}{-}Tc} \underset{k_{-c_2}}{\overset{k_{c_2}}{\leftrightarrow}} \mathrm{TetR^{**}{-}Tc} \underset{k_{-c_3}}{\overset{k_{c_3}}{\leftrightarrow}} \mathrm{TetR^{***}{-}Tc} \quad (8)$$

However, one cannot exclude that the $[Tc-Mg]^+$ binding can trigger conformational changes with different rates in different parts of the molecule.

When the tetracycline is bound to the TetR wt, TetR W43, or TetR W75 mutants in the absence of Mg^{2+}, the kinetic processes are limited only to the first association step without the following conformational changes in the surroundings of tetracycline or surroundings of the Trp45 and Trp75 residues of the protein. Upon binding of tetracycline in the absence of Mg^{2+} to TetR, the fluorescence of Trp75 as well as Trp43 decreased due to the energy transfer from the tryptophan residue to tetracycline. The rate association constants determined for both mutants of TetR (Table 1) are in reasonable agreement with the values determined by monitoring tetracycline fluorescence. This observation indicates that in solution the presence of Mg^{2+} ions is necessary for inducing the structural relaxation of the protein structure, which occurs within different time scale. However, it has been shown that TetR can bind with high affinity anhydrotetracycline in the absence of Mg^{2+} and it can induce TetR in vitro. This indicates that the induction mechanism must be different for tetracycline and for anhydrotetracycline (*21*, *22*).

The X-ray study of the TetR(D) structure, with and without the inducer, shows (*23*, *24*) that the binding of $[Tc-Mg]^+$ to TetR, followed by direct coordination of Mg^{2+} to the His100 residue, triggers a sequence of conformational changes in the protein, which in consequence lead to rotation of the DNA recognition HTH helices in the N-terminal domain. The binding of $[Tc-Mg]^+$ into tunnel-like cavities in the regulatory C-terminal domain of TetR provides sufficient energy to drive these conformational changes in the protein moiety. To determine the thermodynamic parameters, which describe the mechanism of the inducer interaction with Tet repressor, we used an ultrasensitive VP-ITC titration calorimeter. Both, in the case of TetR wt, as well as in case of the single tryptophan containing mutants, this method shows two equivalent binding sites per TetR dimer characterized by exothermic binding reaction. The association constant of $[Tc-Mg]^+$ binding to TetR, determined by direct ITC measurements and equal to $(9.0 \pm 1.2) \times 10^6\ M^{-1}$, is in good agreement with the results derived from kinetic measurements, namely, $K_a = 7.7 \times 10^6\ M^{-1}$. The consistency of the these value, obtained both from kinetic and thermodynamic studies, strongly supports the noncooperative model of the interaction of $[Tc-Mg]^+$ with TetR. The determined value of K_a is by about 2 orders of magnitude lower than the value of K_a equal to about $10^9\ M^{-1}$ obtained by steady-state fluorescence and equilibrium measurements performed at pH 8.7 and 25 °C (*3*). These discrepancies may result from the differences in the pH values of the buffer used in both measurements. In this study, all the measurements have been performed in Tris-HCl buffer at pH 8.0 and 25 °C. It is known (*25*) that the chelating of Mg^{2+} by tetracycline strongly depends on pH value of the buffer used. Since the p*K* value of protonation of the O12 group at the Mg^{2+} binding site of Tc is equal to about 7.7 (*6*), at pH 8.0 employed in this study only about 50% of the inducer has been loaded by the metal ion, as has been estimated by ITC measurements (data not shown). Indeed, the ITC calorimetric studies of Mg^{2+} binding to tetracycline performed as a function of pH shows that the metal binding site was close to one at a pH value near 9.5 (*26*). Since in the cytoplasm of bacteria the pH value is about 7.8, one can expect that inside the cell only about half of the tetracycline can be loaded by Mg^{2+} and in vivo under physiological conditions there will be a mixture of tetracycline chelated and not chelated by Mg^{2+}. ITC measurements show that tetracycline without Mg^{2+} binds to TetR with association constant $K_a = (7.0 \pm 0.5) \times 10^4\ M^{-1}$, and this value is in agreement with the value $(0.96 \pm 0.05) \times 10^5\ M^{-1}$ determined from the kinetic studies. If one takes into account the association constant value $K_a = 3 \times 10^9\ M^{-1}$ for TeR−$[Tc-Mg]^+$ complex, determined at pH 8.7 by Takahashi et al. (*5*), and the $K_a = 7 \times 10^4\ M^{-1}$ value for TetR−Tc complex, determined by ITC measurements, then the geometric average value of these association constant is equal to $1.4 \times 10^7\ M^{-1}$. This average value is close to the value of $9.0 \times 10^6\ M^{-1}$ that has been determined for the TetR−$[Tc-Mg]^+$ complex by the ITC method at pH 8.0 and further supports the suggestion that under physiological conditions there exists a mixed population of complexes of TetR with $[Tc-Mg]^+$ and free tetracycline.

Our ITC measurements show that binding of tetracycline to Tet repressor is an enthalpy-driven reaction. However, binding of free Tc into TetR is a less favorable enthalpic component than in the case of tetracycline chelate. The more favorable changes in $[Tc-Mg]^+$ enthalpy can result from the chelating of the metal by the TetR His100 residue as well as by three hydrogen bonds with a water molecule in the protein binding site (*8*). This molecular $[Tc-Mg]^+$ restraint can be at least responsible for the observed unfavorable entropy changes. On the other hand, it is known from the X-ray structure studies (*24*) that binding of the $[Tc-Mg]^+$ complex causes a switch from the more dynamic structure of Tet repressor, which can adapt to the DNA operator sequences, to the more restrained form, which abolishes or prevents the specific interactions with DNA operator.

ACKNOWLEDGMENT

We are grateful to Prof. W. Hillen for supplying us with the plasmid for production of Tet repressor. We are also grateful to Dr. P. Kuzmic for providing us with the computer program DynaFit.

REFERENCES

1. Schnappinger, D., and Hillen, W. (1996) Tetracyclines: antibiotic action, uptake, and resistance mechanisms, *Arch. Microbiol. 165*, 359−369.
2. Thanassi, D. G., Suh, G. S. B., and Nikaido, H. (1995) Role outer membrane barrier in efflux-mediated tetracycline resistance of *Escherichia coli*, *J. Bacteriol. 142*, 931−938.
3. Hillen, W., and Berens, C. (1995) Mechanism underlying expression of Tn10-encoced tetracycline resistance, *Annu. Rev. Microbiol. 48*, 345−369.
4. Orth, P., Seanger, W., and Hinrichs, W. (1999) Tetracycline-chelated Mg^{2+} ions initiates helix unwinding in Tet repressor induction, *Biochemistry 38*, 191−198.
5. Takahashi, M., Altschmied, L., and Hillen, W. (1986) Kinetic and equilibrium characterization of Tet repressor-tetracycline complex by fluorescence measurements, *J. Mol. Biol. 187*, 341−348.
6. Berens, C., and Hillen, W. (2003) Gene regulation by tetracyclines. Constraints of resistance regulation in bacteria shape TetR for application in eukaryotes, *Eur. J. Biochem. 270*, 3109−3121.
7. Hinrichs, W., Kisker, C., Duvel, M., Müller, A., Tovar, K., Hillen, W., and Saenger, W. (1994) Structure of the Tet repressor-tetracycline complex and regulation of antibiotic resistance, *Science 264*, 418−420.
8. Orth, P., Cordes, F., Schnappinger, D., Hillen, W., Saenger, W., and Hinrichs, W. (1998) Conformational Changes of the Tet repressor induced by tetracycline trapping, *J. Mol. Biol. 279*, 439−447.
9. Kaszycki, P., Guz, A., Drwięga, M., and Wasylewski, Z. (1996) Tet repressor-tetracycline interaction. *J. Protein Chem. 15*, 607−618.
10. Ettner, N., Müller, G., Berens, C. H., Backes, H., Schnappinger, D., Schreppel, T., Pfleiderer, K., and Hillen, W. (1996) Fast large-scale purification of tetracycline repressor variants from overproducing *Escherichia coli* strains, *J. Chromatogr. A 742*, 95−105.
11. Kedracka-Krok, S., and Wasylewski, Z. (1999) Kinetic and equilibrium studies of Tet repressor-operator interaction, *J. Protein Chem. 18*, 117−125.
12. Altschmied, L., and Hillen, W. (1984) Tet repressor tet operator complex formation induces conformational changes in tet operator DNA, *Nucl. Acids Res. 12*, 2171−2180.
13. Peviani, K., Hillen, W., Ettner, N., Lami, H., Doglia, S. M., Piemont, E., Ellouze, Ch., and Chabbert, M. (1995) Spectroscopic investigation of Tet repressor tryptophan-43 upon specific and nonspecific DNA binding, *Biochemistry 34*, 13007−13015.
14. Gill, S. C., and von Hippel, P. (1989) Calculation of protein extinction coefficients from amino acid sequence data, *Anal. Biochem. 182*, 319−326.
15. Kuzmic. P. (1996) Program DynaFit for the analysis of enzyme kinetic data: application to HIV proteinase, *Anal. Biochem. 237*, 260−273.
16. Motulsky, H., and Christopoulos, A. (2003) *Fitting models to biological data using linear and nonlinear regression. A practical guide to curve fitting*, Graph Pad Software Inc., San Diego, CA, www.graphpad.com.
17. Fersht, A. (1999) *Structure and mechanism in Protein Science. A guide to enzyme catalysis and protein folding*, W. H. Freeman and Company, New York.
18. Wasylewski, Z., Kaszycki, P., and Drwięga, M. (1996) A fluorescence study of Tn10-encoded Tet repressor, *J. Protein Chem. 15*, 45−58.
19. Hansen, D., and Hillen, W. (1987) Tryptophan in α-helix 3 of Tet repressor forms a sequence-specific contact with tet operator in solution, *J. Biol. Chem. 262*, 12269−12274.
20. Chabbert, M., Hillen, W., Hansen, D., Takahashi, M., and Bousquet, J.-A. (1992) Structural analysis of the operator binding domain of Tn10-encoded Tet repressor: a time-resolved fluorescence and anisotropy study, *Biochemistry 31*, 1951−1960.
21. Scholz, O., Schubert, P., Kintrup, M., and Hillen, W. (2000) Tet repressor induction without Mg^{2+}, *Biochemistry 39*, 10914−10920.
22. Leypold, C. F., Marian, D.-T., Roman, C., Schneider, S., Schubert, P., Scholz, O., Hillen, W., Clark, T., and Lanig, H. (2004) How does Mg^{2+} affect the binding of anhydrotetracycline in the TetR protein? *Photochem. Photobiol. Sci. 3*, 109−119.
23. Orth, P., Saenger, W., and Hinrichs, W. (1999) Tetracycline-chelated Mg2+ ion initiates helix unwinding in Tet repressor induction, *Biochemistry 38*, 191−198.
24. Orth, P., Schnappinger, D., Hillen, W., Saenger, W., and Hinrichs, W. (2000) Structural basis of gene regulation by the tetracycline inducible Tet repressor-operator system, *Nat. Struct. Biol. 7*, 215−219.
25. Jogun, K. H., and Stezowski, J. J. (1976) Chemical-structural properties of tetracycline derivatives. 2. Coordination and conformational aspects of oxytetracycline metal ion complexation. *J. Am. Chem. Soc. 98*, 6018−6026.
26. Ohyama, T., and Cowan, J. A. (1995) Calorimetric studies of metal binding to tetracycline. Role of solvent structure in defining the selectivity of metal ion-drug interaction, *Inorg. Chem. 34*, 3083−3086.

BI048548W